95-25

Environment Canada

Water Science and Technology Directorate

Direction générale des sciences et de la technologie, eau

Environnement Canada

Static and dynamic calculation of formation fluid displacement induced by hydraulic fracturing

By:

Andrew R. Piggott

95-25

Management Perspective

Hydraulic fracturing is a method of reservoir stimulation that is frequently applied in the oil and gas industries and has considerable potential for application in conjunction with the remediation of contaminated groundwater. The injection of hydraulic fracturing fluid into a geologic formation displaces the fluids that are distributed within the formation prior to fracturing and, in the case of groundwater remediation, this process may result in the mobilization of the target contaminants. Thus, the application of hydraulic fracturing could conceivably hamper, rather than assist, the remediation effort. A relatively simple mathematical solution that models the process of formation fluid displacement due to hydraulic fracturing has been applied to a variety of fracturing scenarios. This paper describes a more detailed, and considerably more computationally demanding, solution that circumvents a limiting assumption invoked in the formulation of the previous solution. A comparison of selected results computed using these two solutions indicates that the simple solution is accurate for a useful range of formation and hydraulic fracture treatment conditions. The accuracy of this solution enables the routine evaluation of the potential for contaminant mobilization by hydraulic fracturing for settings of realistic complexity.

Static and dynamic calculation of formation fluid displacement induced by hydraulic fracturing

Andrew R. Piggott

National Water Research Institute
867 Lakeshore Road
Burlington, Ontario L7R 4A6, Canada
(905) 336-6245 and Fax (905) 336-4400
Andrew.Piggott@CCIW.Ca

NWRI Contribution Number 95-25

May 1995

Abstract

Hydraulically fracturing a geologic formation results in the displacement of the fluids that are distributed within the formation in response to fracturing fluid loss and poroelasticity effects. This process will limit the application of hydraulic fracturing in conjunction with groundwater contamination remediation if the resulting fluid displacement translates to deleterious mobilization of the target contaminants. A dynamic solution for determining the fluid displacement accompanying hydraulic fracturing is developed and compared to a simpler, static solution. The static solution is shown to be adequate for characteristic formation and fracture treatment parameters

Introduction and Review of the Static Solution

Hydraulic fracturing is a routine method of oil and gas well stimulation that may be equally beneficial when applied in conjunction with groundwater contamination remediation (Murdoch et al., 1991). Fracturing fluid loss to the surrounding formation through the walls of the fracture, and poroelasticity effects associated with the compression of the formation, establish an advective transport regime within the formation and displace the fluids that are initially distributed within the formation. This process of fluid displacement may limit the application of hydraulic fracturing technology as an aid to groundwater contamination remediation as the induced fluid displacement has the potential for the mobilization of the target contaminants.

Piggott and Elsworth (1994a) introduced a procedure for calculating the fluid displacement that accompanies hydraulic fracturing. The solution applies to the particular case of a PKN hydraulic fracture

(Perkins and Kern, 1961; Nordgren, 1972) subject to fracturing fluid loss to the formation at a rate that is equal to the rate of fluid injection, thereby minimizing poroelasticity effects.

Figure 1 illustrates the extension of a PKN hydraulic fracture. Two symmetric fracture segments propagate away from the wellbore with a constant height, H, to a maximum length of $L = L_p$ at the end of fluid injection $t = t_p$. The remaining parameters that regulate fracture extension and fluid displacement are the diffusivity and porosity of the formation section, D and n, the fracturing fluid leakoff coefficient, C_L, and the rate of fracturing fluid injection, Q. The extension of a PKN hydraulic fracture subject to fluid loss at the rate of fluid injection is given by (Nordgren, 1972)

$$L = \frac{Q}{2\pi H C_L}\sqrt{t} \tag{1}$$

where the local rate of fluid loss to the formation through the two opposing fracture walls is

$$q = \frac{C_L}{\sqrt{t-\tau}} \tag{2}$$

in which τ is defined as the time at which the formation is first exposed to fracturing fluid. Fluid flow within the formation occurs in the plane of the x- and y-axes (see Figure 1) and fluid displacement is indexed by the displacement components in the directions of coordinate axes

$$\begin{aligned} \Delta_x &= x_f - x_o \\ \Delta_y &= y_f - y_o \end{aligned} \tag{3}$$

where x_o and y_o and x_f and y_f are the initial and final positions of a reference fluid particle, respectively. The total displacement of the particle is then given by

$$\Delta_T = \sqrt{\Delta_x^2 + \Delta_y^2}\ . \tag{4}$$

The solution for formation fluid displacement reported in Piggott and Elsworth (1994a) is based on the assumption that the displacement of the reference fluid particle is sufficiently small that the velocity that is applied to the particle is unchanged with respect to the motion of the particle. This is referred to as a

static solution, since it assumes that the fluid particle is static with respect to the calculation of velocity. This approximation yields

$$\Delta_x = \frac{Qt_p}{2HL_p n} \int_{-1}^{1} \frac{2}{\pi^2} \sqrt{1-x_{j,d}^2}\ \frac{x_d - x_{j,d}}{r_{j,d}^2}\, dx_{j,d}$$
$$\Delta_y = \frac{Qt_p}{2HL_p n} \int_{-1}^{1} \frac{2}{\pi^2} \sqrt{1-x_{j,d}^2}\ \frac{y_d - y_{j,d}}{r_{j,d}^2}\, dx_{j,d} \qquad (5)$$

with

$$r_{j,d} = \sqrt{(x_d - x_{j,d})^2 + (y_d - y_{j,d})^2} \qquad (6)$$

where geometry is expressed in dimensionless form relative to the length of the fracture at the end of fluid injection, $x_d = x/L_p$ and $y_d = y/L_p$. In (5), integration implies the superposition of displacement increments due to fluid loss along the length of the fracture with $-1 \le x_{j,d} \le 1$ and $y_{j,d} = 0$.

The assumption that the velocity of the fluid particle is everywhere equal to the velocity calculated at the initial location of the particle is an obvious limitation of the static solution. It is expected that the accuracy of the static solution will degrade as the displacement of the particle increases, and that a dynamic solution that explicitly represents the motion of the particle is required for the case of large displacement magnitudes. This paper introduces such a solution, again for a PKN hydraulic fracture subject to high fluid loss, and compares the displacement magnitudes predicted by the static and dynamic solutions as a measure of the adequacy of the static solution.

Formulation of the Dynamic Solution

The dynamic solution is derived through the superposition of velocity increments that correspond to the discretization of fluid loss to the formation with respect to time and position along the length of the fracture. Derivation of the dynamic solution begins with the hydraulic head induced by continuous, point fluid injection as stated by the Theis relation (e.g., Freeze and Cherry, 1979)

$$h = \frac{Q}{4\pi T} \int_u^{\infty} \frac{e^{-u}}{u} du \tag{7}$$

where u is defined as

$$u = \frac{r^2}{4Dt} \tag{8}$$

and Q is the rate of fluid injection, r is the distance between the fluid source and the observation location, T and D are the transmissivity and diffusivity of the formation, and t is time relative to the onset of fluid injection.

From (7) and (8), it can be shown that the advective velocity induced by a finite injection event is

$$v_{r,i,j} = \frac{Q_{i,j}}{2\pi Hn} \frac{1}{r_j} \frac{1}{t-t_i} u_{i,j} e^{-u_{i,j}} \Delta t_i \tag{9}$$

where

$$u_{i,j} = \frac{r_j^2}{4D(t-t_i)} . \tag{10}$$

Here, $Q_{i,j}$, t_i, and Δt_i denote the rate, onset, and duration of the injection event; H and n are the thickness and porosity of the formation; and r_j is the distance between the injection and observation locations (subscripts i and j indicate the timing and position of the injection event, respectively). The geometry of this scenario is depicted in Figure 2. Partitioning the radially directed velocity increment given by (9) into components in the directions of the x- and y-axes yields

$$\begin{aligned} v_{x,i,j} &= \frac{Q_{i,j}}{2\pi Hn} \frac{x-x_j}{r_j^2} \frac{1}{t-t_i} u_{i,j} e^{-u_{i,j}} \Delta t_i \\ v_{y,i,j} &= \frac{Q_{i,j}}{2\pi Hn} \frac{y-y_j}{r_j^2} \frac{1}{t-t_i} u_{i,j} e^{-u_{i,j}} \Delta t_i \end{aligned} \tag{11}$$

The variation of fluid injection with time and position during the period of fracture extension may be determined from (1) and (2) as

$$Q_{i,j} = \frac{Q}{\pi L_p} \frac{1}{\sqrt{t_{i,d} - x_{j,d}^2}} \Delta x_j \tag{12}$$

where time is expressed in dimensionless form relative to the duration of fluid injection, $t_d = t/t_p$, and Δx_j is an increment of fracture length as shown in Figure 2. Substitution of (12) into (11) yields

$$\begin{aligned} v_{x,i,j} &= \frac{Q}{2L_pHn} \frac{1}{\pi^2} \frac{1}{\sqrt{t_{i,d} - x_{j,d}^2}} \frac{x_d - x_{j,d}}{r_{j,d}^2} \frac{1}{t_d - t_{i,d}} u_{i,j} e^{-u_{i,j}} \Delta x_{j,d} \Delta t_{i,d} \\ v_{y,i,j} &= \frac{Q}{2L_pHn} \frac{1}{\pi^2} \frac{1}{\sqrt{t_{i,d} - x_{j,d}^2}} \frac{y_d - y_{j,d}}{r_{j,d}^2} \frac{1}{t_d - t_{i,d}} u_{i,j} e^{-u_{i,j}} \Delta x_{j,d} \Delta t_{i,d} \end{aligned} \tag{13}$$

which describes the velocity contributed by fracturing fluid loss at a particular time and position along the length of the fracture. The velocity resulting from fluid loss over the duration of injection and length of the fracture is obtained by superposition of these velocity increments. In integral form, this translates to

$$\begin{aligned} v_x &= \frac{Q}{2L_pHn} \int_0^{t_{i,d}^*} \int_{-x_{i,d}^*}^{x_{i,d}^*} \frac{1}{\pi^2} \frac{1}{\sqrt{t_{i,d} - x_{j,d}^2}} \frac{x_d - x_{j,d}}{r_{j,d}^2} \frac{1}{t_d - t_{i,d}} u_{i,j} e^{-u_{i,j}} dx_{j,d} dt_{i,d} \\ v_y &= \frac{Q}{2L_pHn} \int_0^{t_{i,d}^*} \int_{-x_{i,d}^*}^{x_{i,d}^*} \frac{1}{\pi^2} \frac{1}{\sqrt{t_{i,d} - x_{j,d}^2}} \frac{y_d - y_{j,d}}{r_{j,d}^2} \frac{1}{t_d - t_{i,d}} u_{i,j} e^{-u_{i,j}} dx_{j,d} dt_{i,d} \end{aligned} \tag{14}$$

Fracturing fluid loss to the formation ceases at the end of fluid injection since the high rate of fluid loss precludes the retention of the fluid within the fracture. Thus, the limits of integration with respect to time are $t_{i,d} = 0$ and $t_{i,d} = t_{i,d}^*$ where $t_{i,d}^*$ is the lesser of the current time and the time at the end of fluid injection. The limits of integration with respect to position are $x_{j,d} = -x_{j,d}^*$ and $x_{j,d} = x_{j,d}^*$ where $x_{j,d}^*$ is the lesser of the current length of the fracture and the length of the fracture at the end of fluid injection.

Equation (14) is an integral equivalent of a system of nonlinear ordinary differential equations and is subject to the initial conditions $x(t) = x_o$ and $y(t) = y_o$ at $t = 0$. The desired output of the dynamic solution are the values $x(t) = x_f$ and $y(t) = y_f$ corresponding to $t \rightarrow \infty$.

Calculation of fluid displacement using the dynamic solution is considerably more intricate and computationally demanding than the analogous exercise using the static solution. This task is further

complicated by the singular behaviour of the integrands in (14) and by the lack of a definite upper bound for the solution of the system of differential equations. The singular behaviour of the integrands may be managed through the application of Gauss-Chebyshev quadrature (Press et al., 1992). An approximate upper bound for the solution of the system of differential equations may be obtained by monitoring the motion of the fluid particle in terms of the characteristic time

$$t_c = \frac{r_i^2}{8D} \tag{15}$$

which is the time to peak velocity assuming instantaneous injection at the wellbore. In this approach, the motion of the particle is determined over increments of the characteristic time and iteration is terminated when the displacement of the particle over an increment is less than a nominal fraction of the calculated, total displacement of the particle.

The dynamic solution was implemented as a FORTRAN algorithm that exploits the IMSL subroutines DGQRUL and DIVPRK (IMSL, 1992) for Gauss-Chebyshev quadrature and evaluation of the system of differential equations, respectively. While carefully programmed for optimal performance, the dynamic solution proceeds many orders of magnitude more slowly than the static solution. This contrast indicates the value of the static solution as an alternative to the dynamic solution.

Comparison of the Static and Dynamic Solutions

A comparison of the static and dynamic solutions was undertaken using the formation and fracture treatment parameters cited in Piggott and Elsworth (1994a). Briefly, these parameters are a formation thickness of H = 45.7 m, a leakoff coefficient of C_L = 0.000393 m/s$^{1/2}$, an injection rate and duration of Q = 0.0795 m^3/s and t_p = 12 000 s, and a fracture length of L_p = 77.0 m. These parameters correspond to hydraulic fracturing performed in the context of hydrocarbon reservoir stimulation and may translate to displacement magnitudes that exceed the values that are characteristic of hydraulic fracturing applied in conjunction with groundwater contamination remediation. In this comparison, the porosity of n = 0.2 cited in Piggott and Elsworth (1994a) was replaced by a range of porosities of n = 10^{-8} to 10^{-1} to illustrate the

impact of varying displacement magnitudes on the static and dynamic solutions. Further, an arbitrary diffusivity of D = 1 m^2/s was assumed following preliminary analyses that indicated that diffusivity regulates the timing of fluid motion, and not the terminal displacement of the particle. Total displacement was determined for the five observation locations indicated in Figures 3 and 4; these observation locations are positioned at $(x_o,y_o) = (0.25L_p,0.25L_p)$, $(0.5L_p,0.5L_p)$, (L_p,L_p), $(2L_p,2L_p)$ and $(4L_p,4L_p)$.

Figure 3 compares the total fluid displacements computed for the five observation locations using the static and dynamic solutions and the indicated range of porosities. Displacement decreases with increasing distance from the wellbore, as indexed by observation locations 1 through 5. The magnitudes predicted by the static and dynamic solutions match precisely for all observation locations for porosities in the range of $n = 10^{-3}$ to 10^{-1}. However, the solutions diverge for decreasing values of porosity, where the departure of the solutions is apparent first for observation locations that are close to the wellbore and subject to relatively large displacement. Thus, displacement magnitude is significant in defining the error associated with the static solution. This is an expected result as the static solution explicitly assumes limited fluid displacement. Significantly, the static solution consistently overestimates the dynamic results at small values of porosity. Evaluating the potential for contaminant mobilization using the static solution is therefore a conservative approach as the static solution either accurately estimates, or overestimates, fluid displacement. It should be noted that the lower end of the indicated range of porosities is plausible only for naturally fractured media and is included to illustrate the departure of the static and dynamic results.

Figure 4 compares the results computed using the dynamic solution to results determined through the assumption that fluid loss to the formation occurs at the wellbore rather than along the length of the fracture. In previous analyses (Piggott and Elsworth, 1994a; Piggott and Elsworth, 1994b), this axisymmetric approximation was shown to be adequate for observation locations positioned at greater than two fracture lengths from the wellbore, $r_i > 2L_p$. The axisymmetric approximation shown in Figure 4 was obtained by relating the total volume of fluid injected into the formation, Qt_p, to the pore volume included between the initial and final positions of the fluid particle, $\pi r_f^2 Hn - \pi r_i^2 Hn$. This allows the total (radial) fluid displacement of the particle to be determined as

$$\Delta_T = \sqrt{r_i^2 + \frac{Qt_p}{\pi H n}} - r_i \,. \tag{16}$$

The relation between the distributed and axisymmetric results noted in the previous analyses is equally apparent in Figure 4, which indicates a close match between the dynamic and axisymmetric results for locations 3, 4 and 5. These observation locations represent $r_i > 1.4L_p$. The axisymmetric approximation also replicates the convergent behaviour of the dynamic results for $n < 10^{-5}$, where the static results differ from the dynamic results at even the most remote observation locations.

Conclusions

The favourable comparison between the static and dynamic solutions indicates that there is a range of formation and fracture treatment conditions where the static solution can be applied in place of the dynamic solution. This outcome has particular relevance for other modes of fracture extension, and for complex formation geometries, where the static solution assumes a much more convoluted form (Piggott and Elsworth, 1994b); for example, three-dimensional fracture propagation where fluid displacement is regulated by multiple hydraulic boundaries. While dynamic solutions can be obtained for these settings, the correspondence between the static and dynamic solutions for plausible conditions, and the fact that the static solution represents a conservative estimate of fluid displacement, favour the use of the static solution as an index of the potential for contaminant mobilization. Indeed, the static calculation of fluid displacement for complex fracture and formation geometries is sufficiently computationally demanding that the additional demands imposed by the dynamic solution would be likely to preclude routine analysis.

References

Freeze, R.A. and J.A. Cherry, Groundwater, Prentice-Hall, Englewood Cliffs, 1979.

IMSL, User's Manual IMSL MATH/LIBRARY® FORTRAN Subroutines for Mathematical Applications, Version 1.1, IMSL, Sugar Land, 1992.

Murdoch, L.C., G. Losonsky, P. Cluxton, B. Patterson, I. Klich, and B. Braswell, Feasibility of hydraulic fracturing to improve remedial actions, USEPA/600/S2-91/012, 1991.

Nordgren, R.P., Propagation of a vertical hydraulic fracture, Society of Petroleum Engineers Journal, 253, 306-314, 1972.

Perkins, T.K. and L.R. Kern, Widths of hydraulic fractures, Journal of Petroleum Technology, 13, 937-949, 1961.

Piggott, A.R. and D. Elsworth, Formation fluid displacement induced by hydraulic fracturing, in Proceedings of the Eighth International Conference on Computer Methods and Advances in Geomechanics, vol. 2, pp. 1627-1632, A.A. Balkema, Rotterdam, 1994a.

Piggott, A.R. and D. Elsworth, Displacement of formation fluids by hydraulic fracturing, NWRI Contribution Number 94-109, 1994b.

Press, W.H., S.A. Teukolsky, W.T. Vetterling and B.P. Flannery, Numerical Recipes in FORTRAN: The Art of Scientific Computing, Second Edition, Cambridge University Press, New York, 1992.

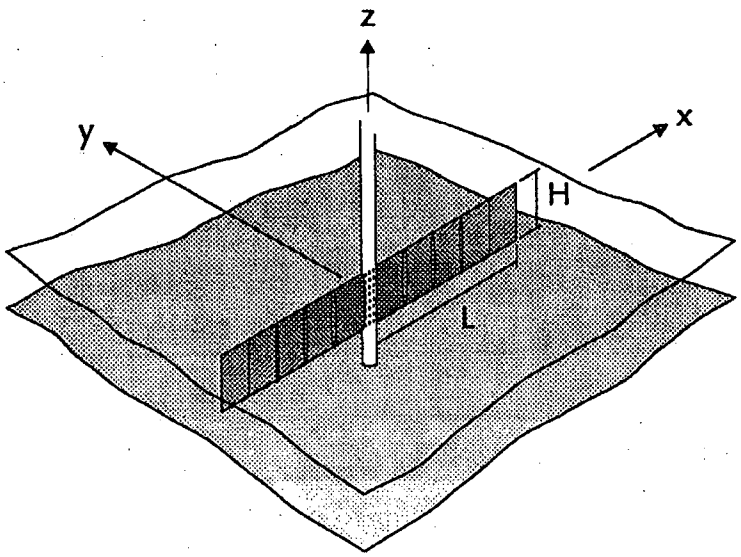

Figure 1. Illustration of the extension of a PKN hydraulic fracture.

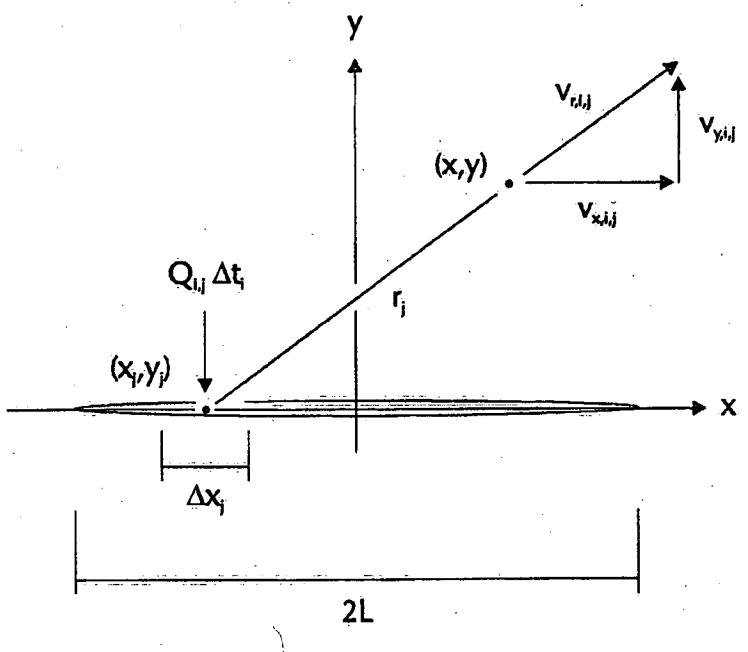

Figure 2. Geometry of the advective velocity resulting from a finite, point injection event.

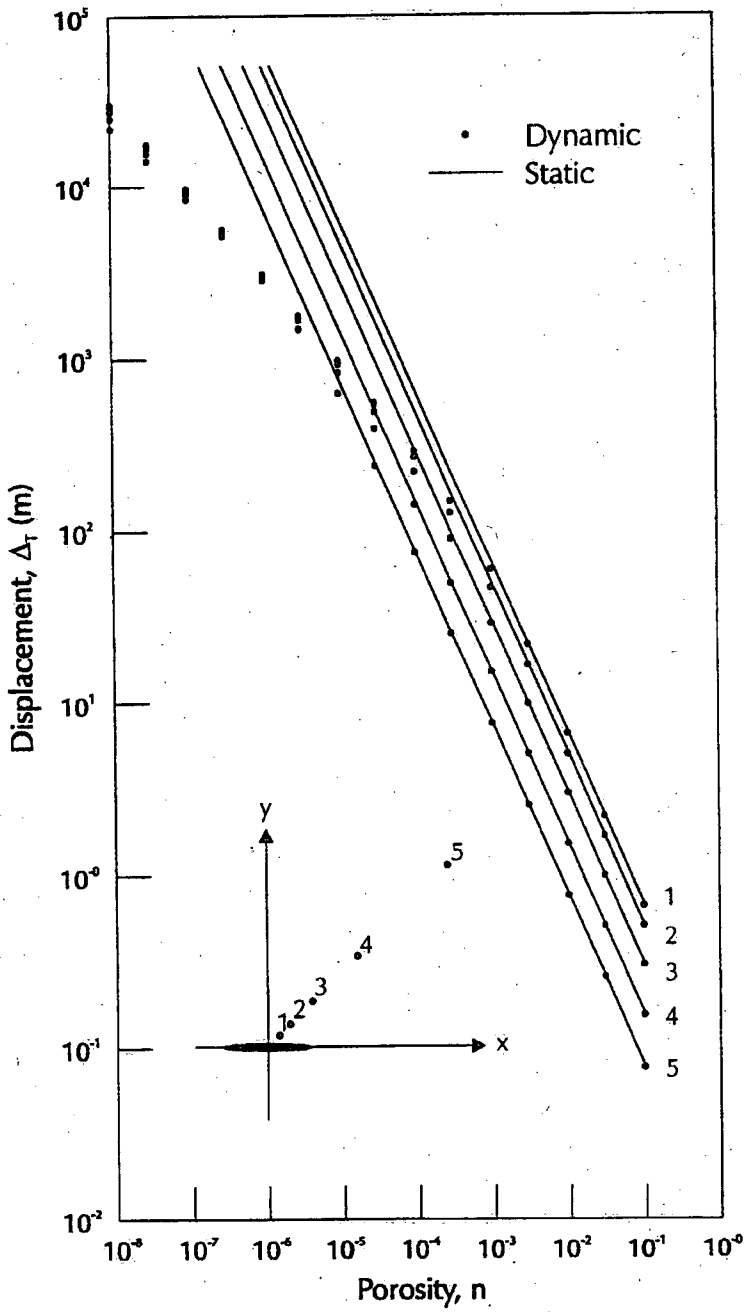

Figure 3. Comparison of the fluid displacement magnitudes predicted using the static and dynamic solutions. Results are shown for the five observation locations indicated in the inset.

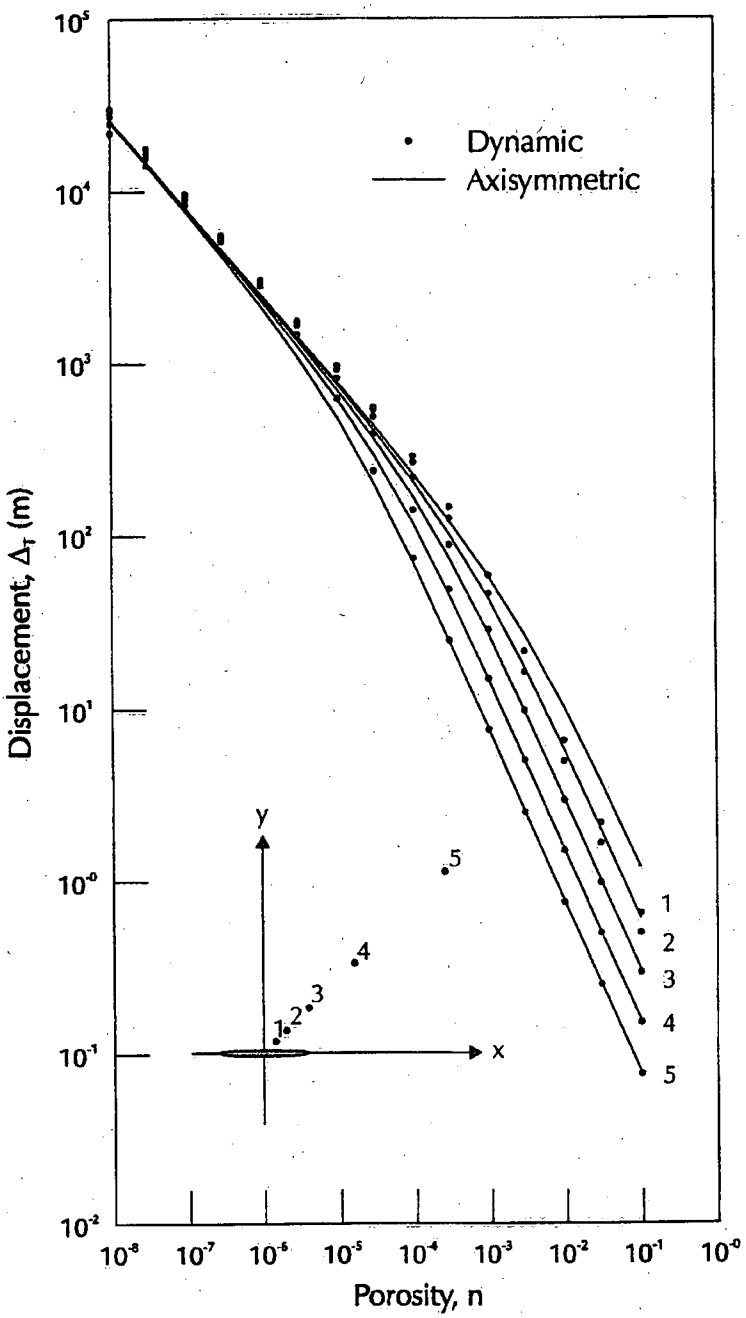

Figure 4. Comparison of the fluid displacement magnitudes predicted using the axisymmetric and dynamic solutions. Results are shown for the five observation locations indicated in the inset.

Environment Canada Environnement Canada

Canada

Canada Centre for Inland Waters
P.O. Box 5050
867 Lakeshore Road
Burlington, Ontario
L7R 4A6 Canada

National Hydrology Research Centre
11 Innovation Boulevard
Saskatoon, Saskatchewan
S7N 3H5 Canada

St. Lawrence Centre
105 McGill Street
Montreal, Quebec
H2Y 2E7 Canada

Place Vincent Massey
351 St. Joseph Boulevard
Gatineau, Quebec
K1A 0H3 Canada

Centre canadien des eaux intérieures
Case postale 5050
867, chemin Lakeshore
Burlington (Ontario)
L7R 4A6 Canada

Centre national de recherche en hydrologie
11, boul. Innovation
Saskatoon (Saskatchewan)
S7N 3H5 Canada

Centre Saint-Laurent
105, rue McGill
Montréal (Québec)
H2Y 2E7 Canada

Place Vincent-Massey
351 boul. St-Joseph
Gatineau (Québec)
K1A 0H3 Canada